Gas-Phase Oxidation of Cm^+ and Cm^{2+} − Thermodynamics of Neutral and Ionized CmO

John K. Gibson,*,† Richard G. Haire,‡ Marta Santos,§ António Pires de Matos,§ and Joaquim Marçalo*,§

Chemical Sciences Division, Lawrence Berkeley National Laboratory, Berkeley, California 94720, USA, Chemical Sciences Division, Oak Ridge National Laboratory, Oak Ridge, Tennessee 37831, USA, and Departamento de Química, Instituto Tecnológico e Nuclear, 2686-953 Sacavém, Portugal

Received: May 30, 2008; Revised Manuscript Received: August 8, 2008

Fourier transform ion cyclotron resonance mass spectrometry was employed to study the products and kinetics of gas-phase reactions of Cm^+ and Cm^{2+}; parallel studies were carried out with $La^{+/2+}$, $Gd^{+/2+}$ and $Lu^{+/2+}$. Reactions with oxygen-donor molecules provided estimates for the bond dissociation energies, $D[M^+-O]$ (M = Cm, Gd, Lu). The first ionization energy, IE[CmO], was obtained from the reactivity of CmO^+ with dienes, and the second ionization energies, $IE[MO^+]$ (M = Cm, La, Gd, Lu), from the rates of electron-transfer reactions from neutrals to the MO^{2+} ions. The following thermodynamic quantities for curium oxide molecules were obtained: IE[CmO] = 6.4 ± 0.2 eV; $IE[CmO^+]$ = 15.8 ± 0.4 eV; D[Cm−O] = 710 ± 45 kJ mol^{-1}; $D[Cm^+-O]$ = 670 ± 40 kJ mol^{-1}; and $D[Cm^{2+}-O]$ = 342 ± 55 kJ mol^{-1}. Estimates for the $M^{2+}-O$ bond energies for M = Cm, La, Gd, and Lu are all intermediate between $D[N_2-O]$ and D[OC−O] − that is, 167 kJ mol^{-1} < $D[M^{2+}-O]$ < 532 kJ mol^{-1} − such that the four MO^{2+} ions fulfill the thermodynamic requirement for catalytic oxygen-atom transport from N_2O to CO. It was demonstrated that the kinetics are also favorable and that the CmO^{2+}, LaO^{2+}, GdO^{2+}, and LuO^{2+} dipositive ions each catalyze the gas-phase oxidation of CO to CO_2 by N_2O. The CmO_2^+ ion appeared during the reaction of Cm^+ with O_2 when the intermediate, CmO^+, was not collisionally cooled − although its formation is kinetically and/or thermodynamically unfavorable, CmO_2^+ is a stable species.

Introduction

Reactions and thermodynamics of elementary gas-phase species enable a better understanding of various fundamental aspects of 5f molecular chemistry as well as provide a basis for developing and validating advanced theoretical methodologies for molecular systems incorporating actinides.[1,2] Such experimental results are also essential for developing advanced technologies and applications in the nuclear industry and for predicting and/or controlling the behavior of actinides in the environment.

Very little thermodynamic information is available for even elementary binary curium oxide molecules.[3,4] Smith and Peterson[5] performed a seminal study of the high-temperature vaporization of Cm_2O_3(s) and estimated $D[Cm-O] \approx 728$ kJ mol^{-1}; although no subsequent quantitative measurements of the dissociation energy of curium monoxide have been reported, recent experiments on the vaporization of curium oxide solids are in accord with these early results.[6,7] Konings has summarized the thermodynamic information available for curium, including an estimate for the enthalpy of formation of CmO(g).[8] Other than the bond energy for CmO provided by Smith and Peterson,[5] there is essentially no experimental thermodynamic information available for curium oxide molecules; a key goal of the present study was to rectify this deficiency. A recent theoretical study of CmO and CmO_2[9] provided estimates for D[Cm−O] and D[OCm−O]; however, without additional experimental validation of the theoretical methodologies employed for actinide-containing molecules, the reliability of such computed bond energies for heavy element molecules remains uncertain.

TABLE 1: Energetics of Monopositive Metal Ions[a]

	ground-state configuration	excited reactive-state configuration(s), [excitation energy given in brackets[b]]	IE[M^+] (eV)[c]
Cm^+	$5f^7 7s^2$	$5f^7 6d7s$ [0.50 eV]; $5f^7 6d^2$ [1.84 eV]	12.4
Gd^+	$4f^7 5d6s$	$4f^7 5d^2$ [0.50 eV]	12.09
Lu^+	$4f^{14} 6s^2$	$4f^{14} 5d6s$ [1.46 eV]; $4f^{14} 5d^2$ [3.64 eV]	13.90

[a] The closed shell xenon and radon core electronic configurations are not included. The energies for Cm^+ are from ref 16. Those for Gd^+ and Lu^+ are from ref 17. [b] 1 eV = 96.485 kJ mol^{-1}. [c] Value for Cm^+ is from ref 18 values for Gd^+ and Lu^+ are from ref 17.

We have previously employed Fourier transform ion cyclotron resonance mass spectrometry (FTICR/MS) to study oxidation reactions of $Pa^{+/2+}$, $Np^{+/2+}$, $Pu^{+/2+}$, and $Am^{+/2+}$.[10–14] In that work, bond dissociation energies, $D[M^{+/2+}-O]$ and/or $D[OM^{+/2+}-O]$, were estimated from the observed oxidation reactions, and ionization energies, $I[MO^{0/+}]$ and/or $I[MO_2^{0/+}]$, were obtained from either electron-transfer reactions, or reactions with dienes.[15] In the present work, we extended these studies to the next member of the actinide series, curium. Studies with representative lanthanide ions, particularly $Gd^{+/2+}$ (the 4f electron counterpart of Cm) and $Lu^{+/2+}$, were carried out for comparison with the results for $Cm^{+/2+}$. Aspects of the chemistry of these metal ions are evaluated in the framework of their atomic energetics − the ground-state configurations for Cm^+, Gd^+, and Lu^+ are given in Table 1, together with the promotion

* To whom correspondence should be addressed. E-mail: JKGibson@lbl.gov (J.K.G.), jmarcalo@itn.pt (J.M.).
† Lawrence Berkeley National Laboratory.
‡ Oak Ridge National Laboratory.
§ Instituto Tecnológico e Nuclear.

10.1021/jp8047899 CCC: $40.75
Published on Web 10/16/2008

TABLE 2: Reaction Products and Kinetics for M^+ Ions with Oxidants[a]

	N_2O	C_2H_4O	H_2O	O_2	CO_2	NO	CH_2O
Cm^+	CmO^+ 0.17 [1.20]	CmO^+ 0.26 [4.49]	CmO^+ 0.049 [1.07]	CmO^+ 0.37 [2.03]	CmO^+ 0.080 [0.53]	CmO^+ 0.013 [0.081]	NR
Gd^+	GdO^+ 0.46 [3.32]	GdO^+ 0.32 [5.64]	GdO^+ 0.089 [2.11]	GdO^+ 0.61 [3.47]	GdO^+ 0.22 [1.46]	GdO^+ 0.16 [1.02]	GdH_2^+ (55) GdO^+ (25) $GdOCH_2^+$ (20) 0.088 [2.12]
Lu^+	LuO^+ 0.21 [1.48]	LuO^+ (85) $LuOH^+$ (10) $LuOH_2^+$ (5) 0.35 [6.08]	LuO^+ 0.033 [0.79]	LuO^+ 0.12 [0.66]	LuO^+ 0.013 [0.09]	NR	NR

[a] Where more than one product was observed, the relative yields are given in parentheses as percentages. The pseudofirst-order rates are expressed as reaction efficiencies, k/k_{COL}, and in brackets as the absolute rates, $k/10^{-10}$ $cm^3molecule^{-1}$ s^{-1}. The absolute rates are considered to be accurate to within ± 50%, and the relative values for comparative purposes to within ± 20%. NR indicates no reaction within the detection limit: $k < 1 \times 10^{-12}$ cm^3 $molecule^{-1}$ s^{-1} ($k/k_{COL} < 0.001$).

energies for attaining divalent state configurations, as well as the second ionization energies.

Experimental Section

The experimental details have been provided elsewhere,[10–14,19,20] and only a brief summary is included here. Ions were produced by laser desorption/ionization (LDI) using the fundamental 1064 nm wavelength of a Spectra-Physics Quanta-Ray GCR-11 Nd:YAG laser. The LDI targets were dilute alloys of the f-block metal in platinum. For example, the curium target was ~5 at% curium in platinum. The curium-248 isotope used in this work was produced in the high-flux isotope reactor at ORNL; it has an alpha emission half-life of 3.5×10^5 years.

Ions emitted from the targets by LDI entered the source cell of a Finnigan FT/MS 2001-DT FTICR/MS equipped with a 3 Telsa magnet and controlled by a Finnigan Venus Odyssey data system; all experiments were carried out in the source cell. With the exception of CH_2O, which was prepared according to a literature procedure,[21] the reactant gases were commercial products. The purities of the gases were confirmed to be >99% from electron ionization mass spectra. The gases were introduced into the spectrometer through a leak valve to pressures of ca. 10^{-8} to 10^{-7} Torr; for some experiments, an initial oxidation step was accomplished by an oxidant gas introduced through pulsed valves. Pressures were measured with a calibrated [22–25] Bayard−Alpert-type ionization gauge. Isolation of the reactant ions was achieved by ejection of other ions using single-frequency, frequency sweep, or SWIFT excitation.[26] Unless otherwise noted, the reactant ions were cooled by collisions with argon, and their thermalization was confirmed by reproducibility of reaction kinetics and product distributions, as well as by the linearity of the pseudo first-order reactant ion decay plots.

Pseudo first-order reaction rate constants, k, were determined from the decay of the reactant ion signals as a function of time at constant neutral reagent pressures. Each reaction was studied for sufficiently long reaction times that less than 10% of the reagent ion remained; the linearity of the kinetic plots over this range established that the ion population was effectively thermalized. Reaction efficiencies are reported as k/k_{COL}, where k_{COL} is the collisional rate constant derived from the modified variational transition-state/classical trajectory theory of Su and Chesnavich.[27] Uncertainties of ± 50% are assigned to the absolute rate constants; relative uncertainties in the reported rate constants, k and k/k_{COL}, are estimated as ± 20%.

Results and Discussion

Reactions of $M^+$and MO^+ with Oxidants: An Evaluation of D[Cm^+−O]. The bare and oxo-ligated metal ions, M^+ and MO^+ where M = Cm, Gd or Lu, were reacted with several oxidants under bimolecular reaction conditions. Under the low-energy conditions of these experiments, if an oxidation or other reaction is observed it must be exothermic (or thermoneutral) − that is, $\Delta_r H \geq 0$. Accordingly, the occurrence of a reaction can be used to establish a lower thermodynamic limit. For some reactions, there may a direct correlation between reaction efficiencies and the degree of exothermicity, but such a correspondence is not necessarily general. Furthermore, non-observation of a reaction may be due to inefficient kinetics and therefore does not necessarily indicate that the absent reaction is endothermic. However, as discussed below, in some cases it is reasonable to infer thermodynamic information based on nonobservation of certain reactions. The several oxidants, RO, used in the present work exhibit a range of bond energies, BDE[R−O], and reactivities, which are appropriate for evaluating the thermodynamics of f-block metal ion oxidation reactions.

TABLE 3: Bond Dissociation Energies and Ionization Energies of Reagent Molecules (RO)[a]

	BDE[R−O]/kJ mol^{-1}	IE[RO]/eV
N_2O	167.1(1)	12.89(0)
C_2H_4O	354.3(6)	10.56(1)
H_2O	491.0(1)	12.62(0)
O_2	498.4(1)	12.07(0)
CO_2	532.2(2)	13.78(0)
NO	631.6(4)	9.26(0)
CH_2O	751.5(1)	10.88(1)
CO	1076.4(1)	14.01(0)

[a] BDEs are from ref 28. IEs are from ref 29. The uncertainty in the final figure is in parentheses.

The results for reactions of M^+ ions with oxidants are summarized in Table 2. The bond energies and ionization energies of the oxidants are given in Table 3. The reactivity of Gd^+ and Lu^+ (and other lanthanide cations) with several oxidants − N_2O,[30] O_2,[30] NO,[31] D_2O,[32] and CO_2[33] − have been previously studied by Bohme and co-workers using an inductively coupled plasma/selected-ion flow tube (ICP/SIFT) tandem mass spectrometer with concurrent results.

As observed reactions must be exothermic (or thermoneutral) under low-energy experimental conditions, these oxidation reactions establish the following lower limits for the M^+−O bond energies: D[Cm^+−O] ≥ D[N−O] = 631.6 kJ mol^{-1}; D[Gd^+−O] ≥ D[H_2C−O] = 751.5 kJ mol^{-1}; and D[Lu^+−O] ≥ D[OC−O] = 532.2 kJ mol^{-1}. The literature values for D[Gd^+−O] = 732 ± 15 kJ mol^{-1} and D[Lu^+−O] = 520 ± 15 kJ mol^{-1}[34] are slightly below these new lower limits; there is no experimental value for D[Cm^+−O].

In contrast to the requirement of exothermicity for the occurrence of an ion-neutral reaction, the nonobservation of an

oxidation reaction may alternatively be due to kinetic hindrance factors and thus does not necessarily indicate endothermicity and does not a priori establish an upper limit for the bond energy. However, previous studies regarding metal ion oxidation with the same oxidants as employed here have indicated that some generalizations can be inferred regarding the kinetics for oxygen-atom transfers to metal ions.[10,11] In particular, oxidations by N_2O, H_2O, and CO_2 often exhibit substantial activation barriers; in contrast, C_2H_4O, O_2, NO, and CH_2O are generally relatively facile oxygen-atom donors. Accordingly, from the experimental results we tentatively propose the following upper limits: $D[Cm^+-O] \leq D[H_2C-O] = 751.5$ kJ mol^{-1}; and $D[Lu^+-O] \leq D[N-O] = 631.6$ kJ mol^{-1}. Furthermore, the observation that oxidation of Cm^+ by NO proceeds quite inefficiently (Table 2) suggests this reaction is within <100 kJ mol^{-1} of the thermodynamic threshold of 631.6 kJ mol^{-1}. Accordingly, we estimate $D[Cm^+-O] = 670 \pm 40$ kJ mol^{-1}. Considering the previous literature values,[34] as well as the kinetics measured in the present work, we also arrive at the following estimates: $D[Gd^+-O] = 780 \pm 30$ kJ mol^{-1}; and $D[Lu^+-O] = 560 \pm 30$ kJ mol^{-1}.

Under thermal conditions, both CmO^+ and GdO^+ were unreactive toward N_2O, O_2, CO_2, NO, and CH_2O; LuO^+ was unreactive with the first three of these oxidants (the reactions of LuO^+ with NO and CH_2O were not studied). As the highest common oxidation state for Cm, Gd, and Lu is M(III), it is not surprising that oxidation does not readily occur to the MO_2^+, in which the formal oxidations states would be assigned as M(V). With H_2O, each of the three MO^+ exhibited inefficient addition reactions to give $CmO_2H_2^+$, $GdO_2H_2^+$, and $LuO_2H_2^+$. These addition products may be adducts, $MO^+ \cdot H_2O$, or bis-hydroxides, $M(OH)_2^+$, where the trivalent oxidation states of the metal centers are retained. Reactions of the MO^+ with ethylene oxide revealed distinctive behaviors discussed below.

Although oxidation of CmO^+ did not occur after collisionally cooling, oxidation to CmO_2^+ by O_2 did occur in the Cm^+/O_2 reaction sequence when the CmO^+ intermediate was not thermalized. This observation can be attributed to the oxidation of a nascent excited-state CmO^+, denoted as CmO^+*, according to eqs 1a and 1b.

$$Cm^+ + O_2 \rightarrow CmO^{+*} + O \quad (1a)$$

$$CmO^{+*} + O_2 \rightarrow CmO_2^+ + O \quad (1b)$$

As the secondary CmO_2^+ product appears only in the absence of cooling of the intermediate CmO^+*, eq 1b is evidently thermodynamically and/or kinetically hindered under thermal conditions. The occurrence of eq 1b demonstrates that CmO_2^+ is an intrinsically stable species, which evidently resides at a local energy minimum on the potential energy surface.

Reactions of MO^+ with Dienes: Evaluations of IE[CmO] and D[Cm−O]. Cornehl et al.[15] identified a correlation between the electron affinities of LnO^+ (EA[LnO^+]) and the efficiencies of these ions in activation of 1,3-butadiene (C_4H_6) and isoprene (C_5H_8). The correlation was presented in the framework of IE[LnO], which are equivalent to EA[LnO^+] and thus the electrophilicities of the metal oxide ions. It was subsequently established that a similar behavior appeared for AnO^+ with these dienes: the greater the IE[AnO], the more efficient the reaction with a given diene substrate.[11] Although the same correlation of reactivity with EA[MO^+] was exhibited within both the lanthanide and actinide series, evidently there is a reactivity offset between the two series such that, for LnO^+ and AnO^+ ions with similar EAs, the absolute reactivity of the LnO^+ ion is greater than that of the AnO^+ ion. In particular, the onset of reactivity with isoprene appears for TbO^+ (EA ≈ 5.6 eV) among the LnO^+ ions,[15] and for UO^+ (EA = 6.03 eV [35]) among the AnO^+ ions.[11] The evident requirement for a higher EA for the actinide oxide ions may reflect the generally greater covalent contribution to bonding in actinide complexes.[36] Such a greater covalency should reduce the effective charge on the metal center, thereby generally diminishing the efficacy of electrophilic attack of AnO^+ ions compared with more ionic LnO^+ ions.

TABLE 4: Reaction Products and Kinetics for MO^+ and Cm^+ with Butadiene and Isoprene[a]

	1,3-C_4H_6	C_5H_8
CmO^+	NR	$CmOC_3H_4^+$ (50) $CmOC_5H_6^+$ (50) 0.19 [1.96]
GdO^+	NR	$GdOC_3H_4^+$ (60) $GdOC_5H_6^+$ (40) 0.11 [1.24]
LuO^+	$LuOC_2H_2^+$ (50) $LuOC_2H_4^+$ (35) $LuOC_4H_4^+$ (15) 0.20 [2.14]	$LuOC_3H_4^+$ (50) $LuOC_5H_6^+$ (50) 0.33 [3.50]
Cm^+	$CmC_2H_2^+$ (85) $CmC_4H_4^+$ (5) $CmC_4H_6^+$ (10) 0.18 [1.84]	$CmC_2H_2^+$ (20) $CmC_3H_4^+$ (50) $CmC_5H_6^+$ (30) 0.22 [2.27]

[a] Results are presented as described in footnote (a) of Table 3.

Because the ThO^+ ion distinctively produces the radical-like $ThOC_5H_5^+$ product in its reaction with isoprene,[11] the reactivity of UO^+ with dienes is considered to better represent the characteristic electrophilic attack mechanism seen with the LnO^+.[37] Accordingly, IE[UO] = 6.0313 ± 0.0006 eV[35] is used as the benchmark for evaluating the IE[AnO] based on reactivities of AnO^+ with dienes.[11,12] The results for reactions of CmO^+ with dienes are given in Table 4. Other than inefficient adduct formation with ThO^+[11] and significant reactivity with PaO^+, which constitutes a special case in the An series,[37] no other AnO^+ ions (An = U, Np, Pu, Am, Cm) reacted with butadiene.[11] The reaction efficiencies with isoprene ranged from $k/k_{COL} = 0.01$ for NpO^+ and PuO^+,[11] up to 0.19 for CmO^+ as measured in the present work. Although the reaction efficiency of UO^+ with isoprene ($k/k_{COL} = 0.02$[11]) was apparently slightly greater than for NpO^+ and PuO^+, dehydrogenation was induced by the latter two ions whereas UO^+ exhibited only adduct formation: thus, the intrinsic reactivity of UO^+ is considered slightly lower than of NpO^+ and PuO^+. The overall order of AnO^+ reactivities with dienes is assigned as follows, with the IE[MO]/eV given in parentheses:

$$ThO^+(6.60) > CmO^+(6.4 \pm 0.2) > AmO^+(6.2 \pm 0.2) > NpO^+(6.1 \pm 0.2) \approx PuO^+(6.1 \pm 0.2) \geq UO^+(6.03)$$

The values for IE[ThO] and IE[UO] are from Heaven and co-workers;[35,38] the IE[AmO], IE[NpO], and IE[PuO] were obtained previously from diene reactivities.[11,12] The assigned IE[CmO] = 6.4 ± 0.2 eV is based on the observation that both CmO^+ and AmO^+ are inert toward butadiene but the reactivity with isoprene is greater for CmO^+ ($k/k_{COL} = 0.19$) than AmO^+ ($k/k_{COL} = 0.04$ eV[11]). This new estimate for IE[CmO] = 6.4 ± 0.2 eV is in accord with a qualitative prediction[39] that IE[CmO] > IE[Cm] = 5.9914 eV.[40] Although the comparative reactivity of ThO^+ was not used as a benchmark per se, inclusion of its reactivity in the present evaluation is consistent with the comparative ionization energies. In a recent theoretical study,[9]

IE[AmO] = 6.3 eV was obtained, in good agreement with the experimental value, 6.2 ± 0.2 eV, previously obtained using the diene reactivity method.[11,12]

Using the $D[CmO^+] = 670 \pm 40$ kJ mol^{-1} estimated above, IE[CmO] = 6.4 ± 0.2 eV, and IE[Cm] = 5.9914 eV,[40] we obtain $D[CmO] = D[CmO^+] - IE[Cm] + IE[CmO] = 710 \pm 45$ kJ mol^{-1}. This value is in good agreement with the value of 728 kJ mol^{-1} reported by Smith and Peterson,[5] as well as with a more recent estimate of 709 kJ mol^{-1}.[41] Konings[8] has presented thermodynamic estimates for curium and its oxides. Using $\Delta H_f[Cm(g)] = 384 \pm 10$ kJ mol^{-1} and $\Delta H_f[CmO(g)] \approx -175$ kJ mol^{-1} from ref 8 and $\Delta H_f[O(g)] = 249$ kJ mol^{-1},[28] $D[CmO] \approx 808$ kJ mol^{-1} is derived, which is ~100 kJ mol^{-1} higher than the value deduced from our experimental results; accordingly, we suggest that the actual value for $\Delta H_f[CmO(g)]$ may be less negative than −175 kJ mol^{-1}.[8] A recent theoretical treatment[9] provided a computed value of D[Cm−O] = 685 kJ mol^{-1}, which is in rather good agreement with our experimental value of 710 ± 45 kJ mol^{-1}.

Results for the reactions of GdO^+ and LuO^+ with dienes are included in Table 4. Our results are in qualitative accord with those for LuO^+/butadiene and GdO^+/isoprene from Cornehl et al.[15] − in particular, the reactivity of LuO^+ was substantially greater than that of GdO^+. However, our k/k_{COL} values are evidently approximately four times lower than those reported previously.[15] Given this discrepancy, it should be emphasized that our evaluations employ reaction efficiencies obtained under internally consistent experimental conditions, and the relative values are considered accurate to within ± 20%. In the case of LuO^+/butadiene, we did not observe adduct formation as reported previously,[15] but rather H_2 elimination, which is in accord with the high reactivity of LuO^+ toward this substrate.

Results for reactions of the bare Cm^+ ion with butadiene and isoprene are also included in Table 4. These reaction efficiencies with the dienes are intermediate between those reported previously[11,37] for the highly reactive early actinide ions, Th^+, Pa^+, U^+, and Np^+, and the less reactive Pu^+ ion. These comparative reactivities accord with the promotion energy for Cm^+ to the $5f^76d7s$ reactive state for hydrocarbon activation, as has been discussed in detail previously[37] (the pertinent promotion energy for Cm^+ is included in Table 1).

Reactions of MO^+ with Ethylene Oxide. Each of the three MO^+ dehydrogenated C_2H_4O to produce $MO_2C_2H_2^+$ (M = Cm, Gd, Lu); $LuOCH_2^+$ was also produced as a minor (15%) product. The following reaction efficiencies, k/k_{COL}, were measured, with the absolute rate constants, $k/10^{-10}$ cm^3 molecule^{-1} s^{-1}, given in brackets: CmO^+/0.15 [2.58]; GdO^+/0.067 [1.18]; LuO^+/0.34 [5.88]. For comparison, $k/k_{COL} = 0.03$ was previously reported for the reaction of AmO^+ with C_2H_4O, with the dominant (60%) channel also being dehydrogenation to give $AmO_2C_2H_2^+$.[11] Other AnO^+ (An = Th, Pa, U, Np, Pu)[10,14] did not dehydrogenate C_2H_4O but instead were oxidized to the AnO_2^+ ions. Thus, the following comparative H_2-elimination reaction efficiencies were identified for ethylene oxide: $CmO^+ > AmO^+$; and $LuO^+ > GdO^+$. These are the same orderings as exhibited with dienes and, as discussed above, parallel the $EA[MO^+] = IE[MO]$.

The apparent correlation between the MO^+ reaction efficiencies for dienes and ethylene oxide suggests a correspondence between the two reaction mechanisms. For dienes, the proposed mechanism entails electrophilic attack of the MO^+ on the π-electron systems.[15] The IEs of different dienes should be qualitatively indicative of their relative nucleophilicities: the lower the IE of a diene, the greater its electron-donating capability and thus the greater its nucleophilicity. However, as Cornehl et al.[15] remarked, this is somewhat of an oversimplification: "...ionization energies cannot be regarded as a quantitative measure of their nucleophilicity".[15]

TABLE 5: Ionization Energies and Proton Affinities of Selected Neutrals[a]

	IE/eV	PA/eV
C_5H_8 (isoprene)	8.86	8.56
C_4H_6 (1,3-butadiene)	9.07	8.12
C_4H_8 (1-butene)	9.55	NA
C_3H_6 (propene)	9.73	7.79
C_2H_4 (ethylene)	10.51	7.05
C_2H_4O (ethylene oxide)	10.56	8.02
H_2O (water)	12.62	7.16

[a] Ionization energies (IE) and proton affinities (PA) are from ref 29.

SCHEME 1: Postulated Mechanism for Dehydrogenation of Ethylene Oxide by MO^+

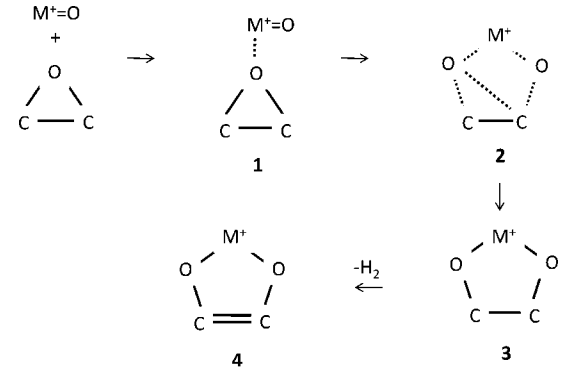

An alternative, perhaps more direct, measure of the nucleophilicity of a molecule is its proton affinity (PA). Ionization energies and proton affinities for some molecules are given in Table 5. It is apparent that small dienes and monoenes exhibit an inverse correlation between IE and PA, so their IEs do indeed provide a qualitative indication of relative nucleophilicities for these similar molecules. In a previous study,[37] it was found that AmO^+ and CmO^+ do not activate ethylene, propene or 1-butene, which is consistent with the greater IEs and lower PAs of the monoenes as compared with the dienes (Table 5) and thus their lower nucleophilicities.

We propose that the reactions of the MO^+ with ethylene oxide proceed by a mechanism in which the rate-determining step entails electron donation from ethylene oxide to the MO^+ − the observed dependence on IE[MO] would be a consequence of this. It is apparent from the IEs and PAs for substrates such as ethylene oxide and water (Table 5) that the IEs do not consistently parallel the PAs, and thus the IEs do not provide a general measure of nucleophilicity. In particular, the IE of ethylene oxide is much greater than that of 1,3-butadiene, but their PAs are quite similar. As remarked by Cornehl et al.,[15] the particular interaction between an electrophilic MO^+ ion, and a nucleophilic neutral substrate will determine the potential energy surface and thus the reaction efficiency. The observation that the MO^+ ions react with ethylene oxide at a comparable

TABLE 6: Reaction Products and Kinetics for M^{2+} with Oxidants

	N_2O[b]	C_2H_4O	H_2O	O_2	CO_2	NO	CH_2O
Cm^{2+}	CmO^{2+} 0.22 [2.99]	CmO^+ 0.26 [8.98]	$CmOH^{2+}$ 0.027 [1.17]	NR	NR	Cm^+ 0.29 [3.61]	CmO^+ 0.013 [0.58]
Gd^{2+}	GdO^{2+} 0.35 [5.11]	GdO^+ 0.28 [9.80]	$GdOH^{2+}$ 0.098 [4.66]	NR	NR	Gd^+ 0.28 [3.53]	GdH^+ (65) GdO^+ (35) 0.12 [5.79]
Lu^{2+}	LuO^{2+} 0.29 [4.12]	Lu^+ (30) LuO^+ (70) 0.27 [9.52]	$LuOH^{2+}$ 0.10 [4.87]	NR	NR	Lu^+ 0.31 [3.96]	Lu^+ (65) LuH^+ (35) 0.23 [10.89]

[a] The results are presented as described in footnote (a) of Table 3. [b] The La^{2+}/N_2O reaction produced LaO^{2+} with the following kinetics: $k/k_{COL} = 0.31$; $k = 4.47 \times 10^{-10}$ cm^3 molecule^{-1} s^{-1}.

TABLE 7: Electron Transfer Kinetics for MO^{2+}[a]

	N_2O (12.89 eV)	CO_2 (13.78 eV)	CO (14.01 eV)
CmO^{2+}	0.38 [5.29]	0.066 [0.86]	0.020 [0.27][b]
LaO^{2+}	0.38 [5.53]	0.13 [1.74]	0.020 [0.27][b]
GdO^{2+}	0.47 [6.73]	0.20 [2.66]	0.050 [0.68]
LuO^{2+}	0.51 [7.20]	0.40 [5.32]	0.041 [0.55]

[a] In each case the product was MO^+ (+ RO^+). The kinetics are presented as described in footnote (a) of Table 2. The IEs of the neutrals from Table 3 are given in parentheses. Reactions of the four MO^{2+} with N_2 (IE = 15.58 eV) and Ar (IE = 15.76 eV) were also studied and no electron transfer reactions were detected. [b] The dominant reaction channels for CmO^{2+} and LaO^{2+} with CO were oxygen-atom transfer to give M^{2+} and CO_2. As a result, the derived minor contributions for the electron transfer channels from CO to CmO^{2+} and LaO^{2+} have a larger uncertainty than is typical (i.e., > 50%).

TABLE 8: Electron Transfer Kinetics for Dipositive Metal Ions[a]

	IE[M^+]	N_2O (12.89 eV)	CO_2 (13.78 eV)	CO (14.01 eV)
Sn^{2+}	14.63 eV	0.01 {1.74 eV}	NR {0.85 eV}	NR {0.62 eV}
Pb^{2+}	15.03 eV	0.11 {2.14 eV}	0.008 {1.25 eV}	0.002 {1.02 eV}
Mn^{2+}	15.64 eV	0.44 {2.75 eV}	0.014 {1.86 eV}	0.017 {1.63 eV}
Ge^{2+}	15.93 eV	0.55 {3.04 eV}	0.22 {2.15 eV}	0.027 {1.92 eV}
Bi^{2+}	16.69 eV	0.40 {3.80 eV}	0.34 {2.91 eV}	0.24 {2.68 eV}

[a] The electron transfer efficiencies, k/k_{COL}, are from refs 13 and 14. The IE[M^+] are from ref 25. The IE[RO] given in parentheses are from ref 29. The exothermicities for electron transfer from RO to M^{2+} (IE[M^+] − IE[RO]) are given in brackets.

efficiency as with the more nucleophilic isoprene substrate − see the PAs in Table 5 − suggests different reaction mechanisms apply for ethylene oxide and dienes, as expected from ab initio considerations. In contrast to an electrophilic attack of the diene π system, a key characteristic of the initial association complex of the MO^+ with C_2H_4O is probably interaction of the oxophilic metal center with the bridging oxo in the neutral molecule, perhaps in concert with electron donation from the neutral C_2H_4O molecule to the MO^+ ion.

For reactions of butadiene with lanthanide oxide ions, it was postulated[15] that the MO^+ ions (M = Ln) add across the terminal carbons to produce a metalla-oxa-cyclohexene intermediate, *cyclo*{−CH_2−CH=CH−CH_2−M^+−O−}, which eliminates H_2 to produce a metalla-oxa-cyclohexadiene product, *cyclo*-{−CH=CH−CH=CH−M^+−O−}. Given the oxophilicity of the metal center, the reaction of an MO^+ with ethylene oxide may proceed by insertion of MO^+ ions into a C−O bond as by a mechanism such as shown in Scheme 1. The initial association **1** might produce the metalla-dioxa-cyclopentane **3**, *cyclo*-{−CH_2−CH_2−O−M^+−O−}, via some indeterminate intermediate(s) as roughly represented by structure **2**. Finally, H_2 elimination from **3** could produce a metalla-dioxa-cyclopentene product **4**, *cyclo*{−CH=CH−O−M^+−O−}. Collision induced dissociation (CID) of $LuO_2C_2H_2^+$ resulted in the following fragmentation products: $LuO_2C_2^+$ (i.e., loss of H_2), $LuOCH_2^+$ (loss of CO), LuO^+ (loss of C_2H_2O), and bare Lu^+. Although these CID results do not provide direct evidence for the postulated metalla-dioxa-cyclopentene, structure **4** in Scheme 1, they are consistent with it.

Reactions of M^{2+} Ions with Oxidants. The ground-state valence electron configurations of the dipositive metal ions are: $5f^8$ for Cm^{2+}, 5d for La^{2+}, $4f^7$5d for Gd^{2+}, and $4f^{14}$6s for Lu^{2+}.[16,17] For each of these M^{2+} ions, the lowest-lying reactive state with two non-f valence electrons is $f^{n-2}d^2$, with the promotion energies to these states estimated as >7 eV.[42] In view of these high promotion energies to a prepared divalent bonding state for the M^{2+} ions, it is expected that the bonds in M^{2+}−O should be much weaker those in M^+−O (the lower promotion energies for the M^+ ions are given in Table 1). Accordingly, the M^{2+} ions were found to be more resistant to oxidation as compared with the M^+ ions.

The results for reactions of the M^{2+} ions with oxidants are summarized in Table 6 (the results for the La^{2+}/N_2O reaction are included as a footnote there). The four M^{2+} ions (M = Cm, La, Gd, Lu) were oxidized to MO^{2+} ions by N_2O. The electronic structures of these MO^{2+} ions are intriguing, as the metal center would be in an unusual, formally tetravalent oxidation state in the M^{2+} = O species. Whereas a Cm(IV) state is known, this oxidation state is not known for the 4f elements investigated here. The implication of oxidation by N_2O is that D[M^{2+}−O] ≥ 167.1 kJ mol^{-1} for all four M^{2+}, in accordance with the thermodynamic assessment below. The result that none of the other oxidants produced MO^{2+} ions (M = Cm, Gd, Lu) is also in accord with our estimates below for D[M^{2+}−O].

With C_2H_4O, the three M^{2+} ions (M = Cm, Gd, Lu) were oxidized concomitant with electron transfer, to produce MO^+. The generic reaction for such an oxidation/electron-transfer is given by eq 2a, and the associated enthalpy by eq 2b:

$$M^{2+} + RO \rightarrow MO^+ + R^+ \quad (2a)$$

$$\Delta H[(2a)/M] = D[R-O] - D[M^+-O] - IE[M^+] + IE[R] \quad (2b)$$

Using the D[M^+−O] values estimated above, 670 ± 40 kJ mol^{-1} for Cm, 780 ± 30 kJ mol^{-1} for Gd, and 560 ± 30 kJ mol^{-1} for Lu; D[O−C_2H_4] = 354.3 kJ mol^{-1};[28] IE[C_2H_4] = 10.51 eV;[29] and the IE[M^+] values given in Table 1, we obtain the following enthalpies from eq 2b for RO = C_2H_4O: ΔH[(2a)/Cm] ≈ −498 kJ mol^{-1}; ΔH[(2a)/Gd] ≈ −578 kJ mol^{-1}; and ΔH[(2a)/Lu] ≈ −533 kJ mol^{-1}. Each of the three observed oxidation/charge separation reactions is quite exothermic. Despite the fact that IE[Cm^+] and IE[Gd^+] are 1.9 and 1.5 eV above IE[C_2H_4O], simple electron transfers to give these bare

M^+ ions were not observed; instead, the much more exothermic oxidation/electron transfer reactions, eq 2a), were overwhelmingly dominant. In contrast, IE[Lu^+] is fully 3.3 eV above IE[C_2H_4O] and accordingly electron transfer to Lu^{2+} was sufficiently exothermic that it was observed as an alternative reaction pathway (Table 6).

It is notable that electron transfer from N_2 did not occur upon oxidation of the M^{2+} ions by N_2O. Evaluation of eq 2b for RO = N_2O (using the D[N_2−O] in Table 2 and IE[N_2] = 15.58 eV[29]) gives the following approximate enthalpies for formation of {$MO^+ + N_2^+$}: ΔH[(2a)/Cm] ≈ −196 kJ mol^{-1}; ΔH[(2a)/Gd] ≈ −276 kJ mol^{-1}; and ΔH[(2a)/Lu] ≈ −231 kJ mol^{-1}. That these exothermic charge-separation exit channels were not observed may be due to activation barriers analogous to those that occur during electron transfer from a neutral to a dipositive ion,[43] which can be understood in terms of Coulombic repulsion between the two emerging monopositive product ions during dissociation of the dipositive encounter complex.

The formation of MOH^{2+} from the M^{2+}/H_2O reactions indicates strong metal hydroxide bonds: D[M^{2+}−OH] ≥ D[H−OH] = 498 kJ mol^{-1}[28] (M = Cm, Gd, Lu). In view of kinetic considerations discussed above, the fact that the charge-separation channel, {$MOH^+ + H^+$}, was not observed does not necessarily imply that IE[MOH^+] ≤ IE[H] = 13.60 eV.[29]

For the reactions of M^{2+} with O_2 (using the D[O−O] in Table 2 and IE[O] = 13.62 eV [29]), eq 2a should be somewhat exothermic, by about −54 kJ mol^{-1} for Cm, about −134 kJ mol^{-1} for Gd, and about −89 kJ mol^{-1} for Lu. None of these three M^{2+} ions exhibited detectable reactivity with O_2, suggesting the presence of an activation barrier. The analogous evaluation for the M^{2+}/CO_2 reactions using eq 2b (using the D[OC−O] and IE[CO] in Table 1) suggests that the nonobserved reactions to produce {$MO^+ + CO^+$} are close to being thermoneutral: ΔH[(2a)/*Cm*] ≈ 18 kJ mol^{-1}; ΔH[(2a)/Gd] ≈ −62 kJ mol^{-1}; ΔH[(2a)/Lu] ≈ −17 kJ mol^{-1}. With NO, both oxidation reactions − to {$MO^{2+} + N$} and to {$MO^+ + N^+$} − should be endothermic for Cm, Gd, and Lu, and these reactions are not observed experimentally. Instead, electron transfers from NO to the M^{2+} ions are exothermic by ≥2.8 eV and occur efficiently for all three M^{2+}.

The reaction pathways for the M^{2+} ions with CH_2O are more diverse due to charge-separation channels enabled by the low ionization energies of the oxygen- and hydrogen-atom donor byproducts: IE[CH_2] = 10.40 eV and IE[CHO] = 8.12 eV.[29] The enthalpies estimated from the charge-separation oxidation reaction, eq 2a, for RO = CH_2O are as follows: ΔH[(2a)/Cm] ≈ −111 kJ mol^{-1}; ΔH[(2a)/Gd] ≈ −191 kJ mol^{-1}; and ΔH[(2a)/Lu] ≈ −146 kJ mol^{-1}. Evidently, formation of CmO^+ by eq 2a with RO = CH_2O is sufficiently exothermic that it occurs, albeit rather inefficiently. As expected from the reaction enthalpies cited above, the formation of GdO^+ is more facile. The alternative hydride-transfer channels appear for the Gd^{2+} and Lu^{2+}ions, but not for the Cm^{2+} ion. The hydride-transfer reaction is given by eq 3a and its enthalpy by eq 3b; IE[CHO] = 8.12 eV[29] and D[H−CHO] = 372 kJ mol^{-1} [28] have been incorporated:

$$M^{2+} + CH_2O \rightarrow MH^+ + CHO^+ \quad (3a)$$

$$\Delta H[(3a)/M] = D[H{-}CHO] - D[M^+{-}H] - IE[M^+] + IE[CHO] = 1155 \text{ kJ mol}^{-1} - D[M^+{-}H] - IE[M^+] \quad (3b)$$

Elkind et al. [44] have reported D[Lu^+−H] = 204 ± 15 kJ mol^{-1}, from which ΔH[(3a)/Lu] ≈ −390 kJ mol^{-1} is obtained; this exothermic channel is observed. Values for D[Cm^+−H] and D[Gd^+−H] have not been reported and are unspecified in the following: ΔH[(3a)/Cm] = −40 kJ mol^{-1} − D[Cm^+−H]; ΔH[(3a)/Gd] = −11 kJ mol^{-1} − D[Gd^+−H]. As the reaction given by eq 3a is observed for gadolinium, it is inferred that D[Gd^+−H] is sufficiently large to drive the reaction. It might be inferred that D[Cm^+−H] is in contrast not sufficiently large, and perhaps D[Cm^+−H] < D[Gd^+−H]. The ground state of Cm^+ is quasi-closed-shell singlet $5f^77s^2$ (Table 1) and promotion − for example to $5f^76d7s$ − is required to form even a two-electron covalent bond, as in a hydride. In contrast, the ground state of Gd^+ is already $4f^75d6s$, suitable for formation of a Gd^+−H bond. The higher promotion energy for Cm^+ may alternatively manifest itself as presenting a kinetic hindrance in hydride-transfer reactions. Finally, IE[Lu^{2+}] = 13.90 eV is sufficiently higher than IE[CH_2O] = 10.88 eV such that efficient electron-transfer occurs to produce bare Lu^+ (+ CH_2O^+).

Each of the MOH^{2+} primary products of the M^{2+}/H_2O reactions (M = Cm, Gd, Lu) reacted efficiently with a second H_2O molecule to give MO^+ according to eq 4:

$$MOH^{2+} + H_2O \rightarrow MO^+ + H_3O^+ \quad (4)$$

The measured efficiencies, k/k_{COL}, and absolute rates, [$k/10^{-10}$ cm^3 molecule^{-1} s^{-1}], for these proton-transfer reactions were as follows: $CmOH^{2+}$/0.57 [24.78]; $GdOH^{2+}$/0.37 [17.73]; $LuOH^{2+}$/0.35 [16.73]. The occurrence of these reactions indicates that PA[MO^+] ≤ PA[H_2O] = 691 kJ mol^{-1}; in view of the activation barriers typically associated with such charge-separation processes, it can be assumed that PA[MO^+] < PA[H_2O] by at least ∼100 kJ mol^{-1}. For comparison, the proton affinity of LaO^+ has been estimated as 482 kJ mol^{-1},[45] which although is remarkably high for a cation is still some ∼200 kJ mol^{-1} lower than PA[H_2O].

Electron Transfer Reactions of MO^{2+}: An Evaluation of IE[CmO^+] and IE[LnO^+] (Ln = La, Gd, Lu). Reactions of four MO^{2+} ions (M = Cm, La, Gd, Lu) with N_2O revealed that oxidation of them did not occur. This contrasts with the behavior of UO^{2+},[13,46] NpO^{2+},[13] PuO^{2+},[13] and PaO^{2+},[14] each of which is efficiently (k/k_{COL} ≥ 0.19) oxidized by N_2O to the corresponding dipositive actinyl ion, AnO_2^{2+}. The behavior of CmO^{2+} and these three LnO^{2+} ions (Ln = La, Gd, Lu) is instead reminiscent of that of ThO^{2+},[13] which is similarly not oxidized by N_2O. The absence of oxidation to MO_2^{2+} by N_2O reflects a common characteristic of these metals in their resistance to form oxidation states as high as M(VI), which is the formal oxidation state in a MO_2^{2+} ion. In contrast to ThO^{2+}, and other early AnO^{2+} ions,[13] the electron affinities of the four MO^{2+} ions studied in the present work are sufficiently high that facile electron transfer from N_2O produces the MO^+ ions.

We previously employed electron transfer (ET) from dipositive ions to neutrals, eq 5a where M^{2+} is a bare or oxo-ligated metal ion and R is a diatomic or triatomic molecule, to estimate ionization energies, and this approach has been described in detail elsewhere.[13,14]

$$M^{2+} + R \rightarrow M^+ + R^+ \quad (5a)$$

$$\Delta_r H^{ET} = IE[R] - EA[M^{2+}] = IE[R] - IE[M^+] \quad (5b)$$

Whereas electron transfer from a neutral to a monopositive ion is generally facile, electron transfer from neutrals to dipositive ions usually exhibits substantial activation barriers. After the onset of electron transfer, its efficiency generally increases with increasing exothermicity. The thermodynamic onset threshold and relative rates for electron transfer can be used to estimate comparative electron affinities of dipositive

SCHEME 2: Catalytic Oxidation of CO by N_2O Mediated by MO^{2+}(M = Cm, La, Gd, Lu)

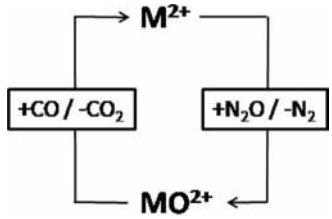

ions. A curve-crossing model has been employed to describe electron transfer to multiply charged ions from neutrals.[47–50] According to this description, electron transfer from a neutral R to a dipositive M^{2+} (eq 5a) will occur if the attractive $M^{2+}-R$ and repulsive M^+-R^+ potential energy curves cross at a sufficiently short distance for resonant electron hopping; this distance is in the approximate range of 0.2−0.6 nm.[48] The maximum curve crossing distance for electron transfer corresponds to a minimum exothermicity for the onset of transfer, $-\Delta_r H^{ET}$.[47,50] Accordingly, the onset of transfer can be used to estimate the difference between the electron affinity of M^{2+} and the ionization energy of R; that is, $-\Delta_r H^{ET}$ [minimum] = $EA[M^{2+}] - IE[R]$ where the minimum enthalpy corresponds to the initial appearance of transfer. Close to the thermodynamic threshold for resonant electron transfer, it is reasonable to presume that the M^+ and R^+ products have minimal internal and translational energies. Favorable alternative reaction pathways can obscure electron transfer onset, as was noted in the preceding section for the reactions of Cm^{2+} and Gd^{2+} with ethylene oxide where electron transfer is substantially exothermic but is not observed because formation of the MO^+ charge-separation products is much more exothermic. To avoid the potential complication of competing exit channels, electron transfer studies are preferably carried out with ion-neutral pairs, which do not otherwise react with one another. The electron transfer investigations reported here are phenomenological and the interpretation of the results is based on comparisons with measured efficiencies for ion-neutral pairs for which $\Delta_r H^{ET}$ is known. This method for estimating unknown $EA[M^{2+}]$ (= $IE[M^+]$) is qualitative, as is reflected in the rather large assigned uncertainties, ± 0.4 eV.

The efficiencies for electron-transfer from neutral molecules to the dipositive metal oxide ions, CmO^{2+}, LaO^{2+}, GdO^{2+}, and LuO^{2+}, were used to estimate the $EA[MO^{2+}] = IE[MO^+]$. The measured electron-transfer kinetics for these MO^{2+} ions are given in Table 7. Estimates for the $IE[MO^+]$ are based on comparison with electron-transfer efficiencies for selected bare calibration M^{2+} ions (M = Sn, Pb, Mn, Ge, Bi). These latter efficiencies for the calibration M^{2+} ions, reported previously,[13,14] are summarized in Table 8. The results in Table 8 suggest that the thermodyanmic onset for electron transfer occurs in the approximate range of 1 eV (from the Pb^{2+}/CO reaction) and 1.2 eV (from the Pb/CO_2 reaction), which is in accord with the estimate of ∼1 eV given by Roth and Freiser.[50]

From a comparison of the relative k/k_{COL} values for the MO^{2+} ions (Table 7) and M^{2+} ions (Table 8), we arrive at the following ordering of second ionization energies:

$$Mn^+ < CmO^+ < LaO^+ < Ge^+ < GdO^+ \approx LuO^+ \ll Bi^+$$

The results with CO in particular suggest that the four $IE[MO^+]$ are fairly close to $IE[Mn^+] = 15.64$ eV and $IE[Ge^+] = 15.92$ eV. We arrive at the following estimates: $IE[CmO^+] = 15.8 \pm 0.4$ eV; $IE[LaO^+] = 15.9 \pm 0.4$ eV; $IE[GdO^+] = 16.0 \pm 0.4$ eV; $IE[LuO^+] = 16.0 \pm 0.4$ eV. As remarked above, the relatively large assigned uncertainties for these values reflect the qualitative nature of the method.

TABLE 9: Thermodynamics of Metal Oxide Molecules[a]

	IE[MO]	$IE[MO^+]$	D[M−O]	$D[M^+-O]$	$D[M^{2+}-O]$
Cm	6.4 ± 0.2	15.8 ± 0.4	710 ± 45	670 ± 40	342 ± 55
La	ND	15.9 ± 0.4	ND	ND	388 ± 50
Gd	ND	16.0 ± 0.4	ND	780 ± 30	403 ± 50
Lu	ND	16.0 ± 0.4	ND	560 ± 30	357 ± 50

[a] These thermodynamic values were derived from the experimental results reported here; ND indicates that this quantity was not determined in the present work. The ionization energies (IE) are in units of eV; the bond dissociation energies (D) are in units of kJ mol^{-1} (1 eV = 96.485 kJ mol^{-1}).

A somewhat lower value of $IE[LaO^+] = 15.2 \pm 0.4$ eV was previously estimated from charge-stripping experiments.[45] However, a recent re-evaluation of the charge-stripping method by Roithová and Schröder indicates that earlier IE assignments from these types of experiments should generally be revised.[51]

We can now estimate the dissociation energies of MO^{2+} to $\{M^{2+} + O\}$ using eq 6:

$$D[M^{2+}-O] = D[M^+-O] + IE[M^+] - IE[MO^+] \quad (6)$$

Employing the $D[M^+-O]$ derived above and $D[La^+-O] = 847 \pm 15$ kJ mol^{-1} from ref 34 (we assign a greater uncertainty of ± 30 kJ mol^{-1} to this latter value); the $IE[M^+]$ in Table 1 and $IE[La^+] = 11.06$ eV from ref 17 and the $IE[MO^+]$ values obtained here, we arrive at the following: $D[Cm^{2+}-O] = 342 \pm 55$ kJ mol^{-1}; $D[La^{2+}-O] = 388 \pm 50$ kJ mol^{-1}; $D[Gd^{2+}-O] = 403 \pm 50$ kJ mol^{-1}; and $D[Lu^{2+}-O] = 357 \pm 50$ kJ mol^{-1}. The estimated dissociation energy for GdO^{2+} in particular suggests that the oxidation of Gd^{2+} to GdO^{2+} by C_2H_4O should be somewhat exothermic; as noted in Table 6, this oxidation process was not observed. Even if oxidation to $\{GdO^{2+} + C_2H_4\}$ is thermodynamically allowed, the observed $\{GdO^+ + C_2H_4^+\}$ exit channel is energetically favored because $IE[C_2H_4] = 10.51$ eV is more than 5 eV below $IE[GdO^+] = 16.0 \pm 0.4$ eV. It should be noted that if $IE[M^+] > IE[O] = 13.62$ eV, then dissociation to $\{M^+ + O^+\}$ is energetically (but not necessarily kinetically) favored over dissociation to $\{M^{2+} + O\}$; that is, $D[M^+-O^+] < D[M^{2+}-O]$. This latter thermodynamic condition evidently applies to LuO^{2+} given the unusually large value of $IE[Lu^+] = 13.90$ eV: $D[Lu^+-O^+] = D[Lu^{2+}-O] - 0.28$ eV = 330 ± 50 kJ mol^{-1}.

Catalytic Oxidation of CO by N_2O Mediated by MO^{2+} (M = Cm, La, Gd, Lu). The $D[M^{2+}-O]$ values derived above, in the range of 342−403 (±50) kJ mol^{-1}, are each intermediate between $D[N_2-O] = 167$ kJ mol^{-1} and $D[CO-O] = 532.2$ kJ mol^{-1}, and thus satisfy the thermodynamic requirement for catalytic oxygen-transfer from N_2O to CO by MO^{2+}: $D[N_2-O] < D[M^{2+}-O] < D[CO-O]$. It was found experimentally that the four MO^{2+} ions − M = Cm, La, Gd, and Lu − each catalyze the gas-phase oxidation of CO by N_2O, according to the sequential oxygen-atom transport reactions (eqs 7 and 8):

$$M^{2+} + N_2O \rightarrow MO^{2+} + N_2 \quad (7)$$

$$MO^{2+} + CO \rightarrow M^{2+} + CO_2 \quad (8)$$

The net reaction for the catalytic cycles is given by eq 9 = eq 7 + eq 8:

$$N_2O + CO \rightarrow N_2 + CO_2 \quad (9)$$

The catalytic cycles are summarized in Scheme 2, where M = Cm, La, Gd, Lu. These cycles were explicitly demonstrated

by the procedure described in detail previously for the analogous catalytic cycle mediated by PaO_2^{2+}.[14] Briefly, the M^{2+} ions were exposed to a mixture of N_2O and CO, the MO^{2+} product from eq 7 was isolated, and the subsequent kinetics were monitored. The concurrent in-growth of M^{2+} − eq 8 − and regeneration of MO^{2+} − eq 7 − was confirmed by a positive deviation from pseudo first-order kinetics for the depletion of MO^{2+}, which demonstrated the regeneration of the MO^{2+} ion, and thus that both eqs 7 and 8 were occurring simultaneously. The result is the overall cycle shown in Scheme 2.

However, the catalytic cycle for each of the four MO^{2+} ions is poisoned by depletion of the MO^{2+} oxygen-atom carriers according to the electron-transfer eqs 10 and 11:

$$MO^{2+} + N_2O \rightarrow MO^{+} + N_2O^{+} \quad (10)$$

$$MO^{2+} + CO \rightarrow MO^{+} + CO^{+} \quad (11)$$

The kinetics for eqs 7, 10, and 11 are given in Tables 6 and 7. The kinetics for eq 8, given as efficiencies, k/k_{COL}, and as $k/10^{-10}$ cm^3 molecule^{-1} s^{-1} in brackets, are as follows: CmO^{2+}/0.26 [3.54], LaO^{2+}/0.21 [2.94], GdO^{2+}/0.16 [2.23], and LuO^{2+}/0.17 [2.30]. Electron transfer from N_2O to the MO^{2+}, to produce inert MO^{+}, proceeds efficiently − $k/k_{COL} \geq 0.38$ (Table 7) − and the catalytic cycles are thus quenched rapidly.

From energetic considerations alone, observation of the exit channel corresponding the right side of eq 8, rather than the charge-separation channel to give $\{M^{+} + CO_2^{+}\}$, would suggest that $IE[M^{+}] \leq IE[CO_2] = 13.78$ eV; in the case of M = Lu, this implication is inconsistent with the literature value, $IE[Lu^{+}] = 13.90$ eV.[17] However, as discussed above, barriers to formation of two monopositive ions from a dipositive ion can be sufficiently large such that energetically favorable charge-separation processes may be so kinetically hindered as to not appear.

Summary and Conclusions

A central goal of the work reported here was to derive thermodynamic estimates for curium oxide molecules based on the kinetics of oxidation, electron-transfer, and diene activation reactions of the bare and oxo-ligated curium cations. The thermodynamic quantities derived in the present work for curium and lanthanide oxides are compiled in Table 9. For the curium oxide molecules, the only value determined previously for comparison is $D[Cm-O] \approx 728$ kJ mol^{-1} from Smith and Peterson,[5] which is in good agreement with our value. A recent theoretical value of $D[Cm-O] \approx 685$ kJ mol^{-1}[9] is also in remarkably good accord. Our suggested values for $D[Gd^{+}-O]$ and $D[Lu^{+}-O]$ in Table 9 are slightly higher than literature values;[34] values are not available for comparison with our $IE[LnO^{+}]$ or $D[Ln^{2+}-O]$ (Ln = La, Gd, Lu).

The $D[M^{2+}-O]$ (M = Cm, La, Gd and Lu) are intermediate between $D[N_2-O]$ and $D[OC-O]$, which is the thermodynamic requirement for oxygen-atom transport from N_2O to CO. It was demonstrated that each of these four MO^{2+} do indeed catalyze the oxidation of CO to CO_2 concomitant with the reduction of N_2O to N_2. There are several examples of such gas-phase oxidation/reduction couples mediated by monopositive metal oxide ions[52] but apparently PaO_2^{2+} is the only dipositive oxide ion to have been shown previously to exhibit such catalytic behavior.[14]

Oxidation of CmO^{+} did not occur with thermalized states. However, CmO^{+} produced from the oxidation of Cm^{+} by O_2 was further oxidized to CmO_2^{+} in the absence of collisional de-excitation. This oxidation is attributed to a thermodynamically and/or kinetically hindered oxidation which proceeds via an excited-state CmO^{+}*. This demonstrates that CmO_2^{+} is a stable albeit elusive species.

Acknowledgment. This work was sponsored by Fundação para a Ciência e a Tecnologia (FCT) and POCI 2010 (cofinanced by FEDER) under contract POCI/QUI/58222/2004; and by the Director, Office of Science, Office of Basic Energy Sciences, Division of Chemical Sciences, Geosciences and Biosciences of the U.S. Department of Energy under Contracts DE-AC05-00OR22725 at ORNL, and DE-AC02-05CH11231 at LBNL. M.S. is grateful to FCT for a Ph.D. grant.

References and Notes

(1) Gibson, J. K. *Int. J. Mass Spectrom.* **2001**, *214*, 1–21.
(2) Gibson, J. K.; Marçalo, J. *Coord. Chem. Rev.* **2006**, *250*, 776–783.
(3) Hildenbrand, D. L. Gurvich, L. V. Yungman, V. S. *The Chemical Thermodynamics of Actinide Elements and Compounds. Part 13: The Gaseous Actinide Ions*; IAEA: Vienna, 1985.
(4) Konings, R. J. M.; Morss, L. R.; Fuger, J. In *The Chemistry of the Actinide and Transactinide Elements,* Third Ed.; Morss, L. R., Edelstein, N. M., Fuger, J., Eds.; Springer: Dordrech, The Netherlands, 2006; pp 2113−2224.
(5) Smith, P. K.; Peterson, D. E. *J. Chem. Phys.* **1970**, *52*, 4963–4972.
(6) Haire, R. G. *J. Alloys Compd.* **1994**, *213/214*, 185–190.
(7) Hiernaut, J. P.; Ronchi, C. *J. Nucl. Mater.* **2004**, *334*, 133–138.
(8) Konings, R. J. M. *J. Nucl. Mater.* **2001**, *298*, 255–268.
(9) Kovács, A.; Konings, R. J. M.; Raab, J.; Gagliardi, L. *Phys. Chem. Chem. Phys.* **2008**, *10*, 1114–1117.
(10) Santos, M.; Marçalo, J.; Pires de Matos, A.; Gibson, J. K.; Haire, R. G. *J. Phys. Chem. A* **2002**, *106*, 7190–7194.
(11) Santos, M.; Marçalo, J.; Leal, J. P.; Pires de Matos, A.; Gibson, J. K.; Haire, R. G. *Int. J. Mass Spectrom.* **2003**, *228*, 457–465.
(12) Gibson, J. K.; Haire, R. G.; Marçalo, J.; Santos, M.; Pires de Matos, A.; Leal, J. P. *J. Nucl. Mater.* **2005**, *344*, 24–29.
(13) Gibson, J. K.; Haire, R. G.; Marçalo, J.; Santos, M.; Pires de Matos, A. *J. Phys. Chem. A* **2005**, *109*, 2768–2781.
(14) Santos, M.; Pires de Matos, A.; Marçalo, J.; Gibson, J. K.; Haire, R. G.; Tyagi, R.; Pitzer, R. M. *J. Phys. Chem. A* **2006**, *110*, 5751–5759.
(15) Cornehl, H. H.; Wesendrup, R.; Harvey, J. N.; Schwarz, H. *J. Chem. Soc., Perkin Trans. 2* **1997**, 2283–2291.
(16) Blaise, J. Wyart, J.-F. *Energy Levels and Atomic Spectra of Actinides: Tables Internationales de Constantes*; Université Pierre et Marie Curie: Paris, 1992; http://www.lac.u-psud.fr/Database/Contents.html.
(17) Martin, W. C. Zalubas, R. Hagan, L. *Atomic Energy Levels−The Rare Earth Elements*; U.S. Department of Commerce: Washington, D.C., 1978.
(18) Morss L. R. In *The Chemistry of the Actinide Elements*, 2nd ed.; Katz, J. J., Seaborg, G. T., Morss, L. R., Eds.; Chapman and Hall: London, 1986; Chap. 17, pp 1278−1360.
(19) Marçalo, J.; Leal, J. P.; Pires de Matos, A. *Int. J. Mass Spectrom. Ion Processes* **1996**, *157/158*, 265–274.
(20) Marçalo, J.; Leal, J. P.; Pires de Matos, A.; Marshall, A. G. *Organometallics* **1997**, *16*, 4581–488.
(21) Perrin,; D. D. Armarego; W. L. F. *Purification of Laboratory Chemicals*, 3rd Ed.;Pergamon Press: Oxford, 1988.
(22) Bruce, J. E.; Eyler, J. R. *J. Am. Soc. Mass Spectrom.* **1992**, *3*, 727–733.
(23) Lin, Y.; Ridge, D. P.; Munson, B. *Org. Mass Spectrom.* **1991**, *26*, 550–558.
(24) Bartmess, J. E.; Georgiadis, R. M. *Vacuum* **1983**, *33*, 149–153.
(25) *CRC Handbook of Chemistry and Physics*, 75th ed.; Lide, D. R., Ed.; CRC Press: Boca Raton, 1994.
(26) Guan, S.; Marshall, A. G. *Int. J. Mass Spectrom. Ion Processes* **1996**, *157/158*, 5–37.
(27) Su, T.; Chesnavich, W. J. *J. Chem. Phys.* **1982**, *76*, 5183–5185.
(28) Lias, S. G. Bartmess, J. E. Liebman, J. F. Holmes, J. L. Levin, R. D. Mallard, W. G., *Gas-Phase Ion and Neutral Thermochemistry*; American Chemical Society: Washington, D.C., 1988.
(29) *Chemistry WebBook - NIST Standard Reference Database Number 69*; Linstrom, P. J., Mallard, W. G., Eds.; National Institute of Standards and Technology: Gaithersburg MD, June 2005; http://webbook.nist.gov.
(30) Cheng, P.; Koyanagi, G. K.; Bohme, D. K. *J. Phys. Chem. A* **2001**, *105*, 8964–8968.
(31) Blagojevic, V.; Flaim, E.; Jarvis, M. J. Y.; Koyanagi, G. K.; Bohme, D. K. *Int. J. Mass Spectrom.* **2006**, *249−250*, 385–391.
(32) Cheng, P.; Koyanagi, G. K.; Bohme, D. K. *ChemPhysChem* **2006**, *7*, 1813–1819.

(33) Cheng, P.; Koyanagi, G. K.; Bohme, D. K. *J. Phys. Chem. A* **2006**, *110*, 12832–12838.
(34) Chandrasekharaiah, M. S. Gingerich, K.A In *Handbook on the Chemistry and Chemistry of Rare Earths*; Gschniedner, K. A., Jr., Eyring, L., Eds.; Elsevier: Amsterdam, 1989; Vol. 12, Chap. 86.
(35) Han, J.; Kaledin, L. A.; Goncharov, V.; Komissarov, A. V.; Heaven, M. C. *J. Am. Chem. Soc.* **2003**, *125*, 7176–7177.
(36) Gaunt, A. J.; Reilly, S. D.; Enriquez, A. E.; Scott, B. L.; Ibers, J. A.; Sekar, P.; Ingram, K. I. M.; Kaltsoyannis, N.; Neu, M. P. *Inorg. Chem.* **2008**, *47*, 29–41.
(37) Gibson, J. K.; Haire, R. G.; Marçalo, J.; Santos, M.; Pires de Matos, A.; Mrozik, M. K.; Pitzer, R. M.; Bursten, B. E. *Organometallics* **2007**, *26*, 3947–3956.
(38) Goncharov, V.; Heaven, M. C. *J. Chem. Phys.* **2006**, *124*, 643121−7.
(39) Gibson, J. K.; Haire, R. G. *J. Phys. Chem. A* **1998**, *102*, 10746–10753.
(40) Erdmann, N.; Nunnemann, M.; Eberhardt, K.; Hermann, G.; Huber, G.; Köhler, S.; Passler, G.; Peterson, J. R.; Trautmann, N.; Waldek, A. *J. Alloys Compd.* **1998**, *271*−*273*, 837–840.
(41) Gibson, J. K. *J. Phys. Chem. A* **2003**, *107*, 7891–7899.
(42) Brewer, L. *J. Opt. Soc. Am.* **1971**, *61*, 1666–1682.
(43) Petrie, S.; Wang, J.; Bohme, D. K. *Chem. Phys. Lett.* **1993**, *204*, 473–480.
(44) Elkind, J. L.; Sunderlin, L. S.; Armentrout, P. B. *J. Phys. Chem.* **1989**, *93*, 3151–3158.
(45) Schröder, D.; Schwarz, H.; Harvey, J. N. *J. Phys. Chem. A* **2000**, *104*, 11257–11260.
(46) Cornehl, H. H.; Heinemann, C.; Marçalo, J.; Pires de Matos, A.; Schwarz, H. *Angew. Chem., Int. Ed. Engl.* **1996**, *35*, 891–894.
(47) Tonkyn, R.; Weisshaar, J. C. *J. Am. Chem. Soc.* **1986**, *108*, 7128–7130.
(48) Gord, J. R.; Freiser, B. S.; Buckner, S. W. *J. Chem. Phys.* **1991**, *94*, 4282–4290.
(49) Gord, J. R.; Freiser, B. S.; Buckner, S. W. *J. Phys. Chem.* **1991**, *95*, 8274–8279.
(50) Roth, L. M.; Freiser, B. S. *Mass Spectrom. Rev.* **1991**, *10*, 303–328.
(51) Roithová, J.; Schröder, D. *Int. J. Mass Spectrom.* **2007**, *267*, 134–138.
(52) Böhme, D. K.; Schwarz, H. *Angew. Chem., Int. Ed.* **2005**, *44*, 2236–2254.

JP8047899